

The Global Variation of Terrestrial Heat Flow

W. H. K. LEE AND GORDON J. F. MACDONALD

*Institute of Geophysics and Planetary Physics
University of California, Los Angeles*

Abstract. Over 900 measurements of surface heat flow have been analyzed in order to obtain the continent-ocean averages and a contour representation. An orthogonal function representation of 757 values yields a global mean of 63.9 ± 3.4 erg cm⁻² sec⁻¹ (1.53 μ cal cm⁻² sec⁻¹). The average over continents is 68.9 erg cm⁻² sec⁻¹ (1.65 μ cal cm⁻² sec⁻¹) and the oceanic average is 62.0 erg cm⁻² sec⁻¹ (1.48 μ cal cm⁻² sec⁻¹). The difference between the continents and oceans is not significant at the 95 per cent confidence level. The contour representation of the heat flows shows certain similarities to the geoid. The correlation is in the sense that where gravity is high the heat flow is low, and vice versa. This correlation is consistent with that expected from convection motions in the upper mantle. An order of magnitude calculation shows that for convection extending over a depth of 1000 km a vertical velocity of 15 cm year⁻¹ is required to explain the associated mass and heat-flow anomalies.

We wish to analyze the terrestrial heat flow in a form which can be directly compared with representations of other fields of geophysical importance. The distributions of the observations are too irregular to yield directly adequate values of the spherical harmonic coefficients. In such a situation, it is perhaps better to make a comparison based on a spatial rather than a spectral representation. A convenient spatial representation is a contour map of the surface heat flow. The objective construction of such a contour map presents a number of problems. The use of functions orthogonal to the station net [Fougere, 1963; G. J. F. MacDonald, unpublished] is particularly well suited to the construction of such contour maps, since the contours are plotted by a digital computer and there is no need to rely on intuition or prejudice.

If the observing stations are on a regular grid, a spherical harmonic analysis will represent the geographical variation of the field, provided that the field does not contain energy at wavelengths less than twice the grid intervals. In practice, all geophysical fields contain energy at short wavelengths and, therefore, there is always the problem of aliasing [Blackman and Tukey, 1958]. A discussion of the question of analyzing data over the surface of the sphere is given by Kaula [1959].

If the stations are irregularly distributed, it is possible to average over degree 'squares' and

use these regularly spaced averages to obtain the spherical harmonic representation. The averaging smooths the values and lowers the energy at wavelengths short compared with the intergrid distance. Such a procedure is unsatisfactory when the data are limited because judgment is required to determine the area over which the smoothing should take place, and the representation must be extrapolated into regions for which no data exist. An alternative scheme of overcoming aliasing is to expand the field in functions orthogonal to the observing stations. The functions are not known a priori, but can be constructed numerically. If there are n determinations scattered over the sphere, a set of n -dimensional basis vectors is generated and orthogonalized and reorthogonalized by the Gram-Schmidt process. The observed vector is expanded in the orthogonal basis. If the stations are irregularly distributed on the surface of the sphere, and if the irregularity is sufficiently great (for example, two-dimensional Poisson distribution), almost all wavelengths are sampled but there is an error in each sample, and this error will be a minimum at a wavelength equal to twice the mean interstation distance. The data are smoothed by truncating the series; the series is truncated objectively by appropriate testing for significance each new function used in the representation. In addition to the advantages of orthogonality, the process is analytic and does not

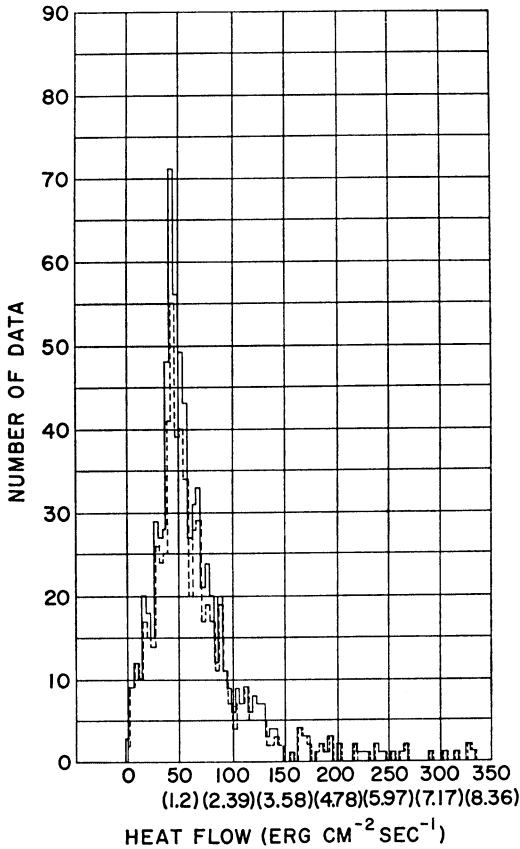


Fig. 2. Histogram of world 757 heat-flow data.

require the extrapolation of values to vacant grid points.

Available heat-flow data. Early in 1963, 687 heat-flow data were compiled and 634 data were analyzed by Lee [1963]. In June 1963, the total number of available data increased to 813 (from over 900 measurements). In reviewing the available data, 56 data were discarded either because the determinations were uncertain or the location of the observation was in doubt [Lee, 1963]. The distribution of the remaining data, 92 in continental areas and 665 in oceans, is shown in Figure 1.

Observations are well distributed over the oceanic areas, but there is a tendency for measurements to be concentrated along anomalous regions such as the east Pacific rise [Von Herzen and Uyeda, 1963] and the mid-Atlantic ridge [Nason and Lee, 1962] (see Figure 1). The large gaps are in the massive continental re-

gions. There are no observations in central Asia, equatorial Africa, or South America.

Histogram of heat-flow data. A histogram of the heat-flow data is shown in Figure 2. The solid line gives the distribution with heat flow of the 757 stations studied in this paper and the dashed line gives the distribution obtained by Lee [1963] using 634 values. In Figure 2, the convention is adopted that will be used throughout the paper. The unit for heat flow used here is $\text{erg cm}^{-2} \text{sec}^{-1}$. However, experimenters report heat flow in microcalories $\text{cm}^{-2} \text{sec}^{-1}$, and we add in parentheses the equivalent microcalorie value. The term *heat flow* is used instead of the proper term *heat flow per unit area*. Since the unit will always be stated, there should be no confusion.

The distribution of heat-flow values with ocean depth is shown in Figure 3. There is some tendency for high values to be associated with a 3000-meter depth, but on the whole there is a low correlation (correlation coefficient = -0.33) of the heat flow in oceans with topography. The data in continental areas are too few to provide an adequate measure of the correlation of heat flow with elevation.

A continent and ocean mean. The arithmetic means and standard errors of the 757 data are listed in the first row of Table 1. The oceanic means are higher than the continental means; the arithmetic mean for the earth of $67.4 \text{ erg cm}^{-2} \text{sec}^{-1}$ (1.61) is significantly higher than the previously accepted mean of $50 \text{ erg cm}^{-2} \text{sec}^{-1}$ (1.2) [Bullard, 1954]. Lee [1963], using the classical method of spherical harmonic analysis, obtained an average value over the sphere of $62.8 \pm 6.3 \text{ erg cm}^{-2} \text{sec}^{-1}$ (1.5), the error being determined by

$$\epsilon = t(P, \nu) \left\{ \left[\sum_{i=1}^N (\Delta_i)^2 \right] / N\nu \right\}^{1/2} \quad (1)$$

$$\Delta_i = h_i - h_e$$

where h_i is the observed value of the heat flow at the i th station, h_e is a value calculated using an expansion, N is the number of grid points used in the analysis, ν is the number of degrees of freedom and is equal to N minus the number of coefficients or functions used in the representation, t is a function of the probability P and the degrees of freedom ν , P is the probability of having $t \geq t(P, \nu)$ by chance for ν

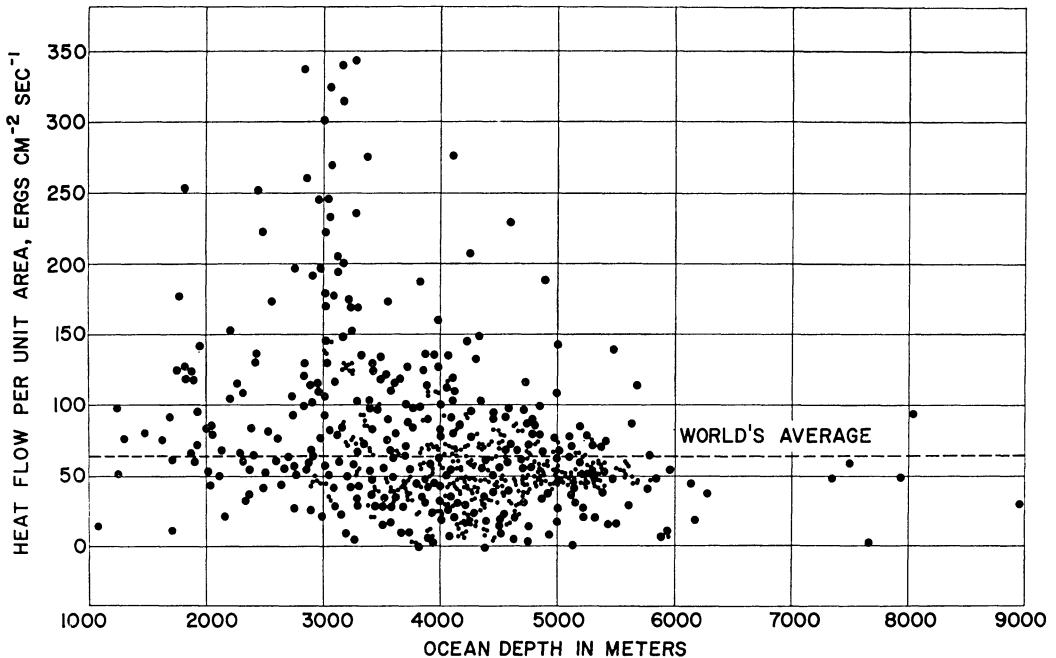


Fig. 3. Scatter diagram showing the distribution of heat flow with ocean depth.

degrees of freedom (the Student t test). The error is calculated on the basis of 95 per cent confidence.

The orthogonal function representation of the 757 values yields a mean of 63.9 ± 3.4 erg $\text{cm}^{-2} \text{sec}^{-1}$ (1.53) for the mean heat flow over the earth. The error is determined according to (1). The orthogonal function representations of averages for the grids given in Table 1 are completely equivalent to the classical spherical harmonic analysis since the values are at grid points. The means obtained from orthogonal representation of all values and from expansion of the averages are close, and we adopt a mean

of 64.0 ± 4.0 erg $\text{cm}^{-2} \text{sec}^{-1}$ (1.53) as the best estimate of the mean for the heat flow. In Figure 3, the orthogonal function representation of all values is shown. The 5° weighted average representation is given in Figure 4, while Figure 5 displays the expansion of the 45° weighted averages.

The standard deviation for a single observation is 48.7 erg $\text{cm}^{-2} \text{sec}^{-1}$ (1.16). To observe the effect of the extreme values, we calculate the mean with all values less than 116 erg $\text{cm}^{-2} \text{sec}^{-1}$ (2.77) and greater than 18.7 erg $\text{cm}^{-2} \text{sec}^{-1}$ (0.45). The resulting mean is 58.7 erg $\text{cm}^{-2} \text{sec}^{-1}$ (1.40).

TABLE 1. Mean Heat Flow over Continents and Oceans (erg $\text{cm}^{-2} \text{sec}^{-1}$)

	Earth	Continents	Oceans
Arithmetic means	67.4 ± 1.8 (1.61)	61.9 ± 2.6 (1.48)	68.2 ± 2.0 (1.63)
Spherical harmonic representation [Lee, 1963]	62.8 ± 6.3 (1.5)		
Orthogonal function representation of all values	63.9 ± 3.4 (1.53)	68.9 (1.65)	62.0 (1.48)
Orthogonal function representation of weighted averages for the $5^\circ \times 5^\circ$ grid	64.0 ± 3.8 (1.53)	67.8 (1.62)	62.4 (1.49)
Orthogonal function representation of weighted averages for the $45^\circ \times 45^\circ$ grid	63.1 ± 6.1 (1.51)	68.2 (1.63)	61.1 (1.46)

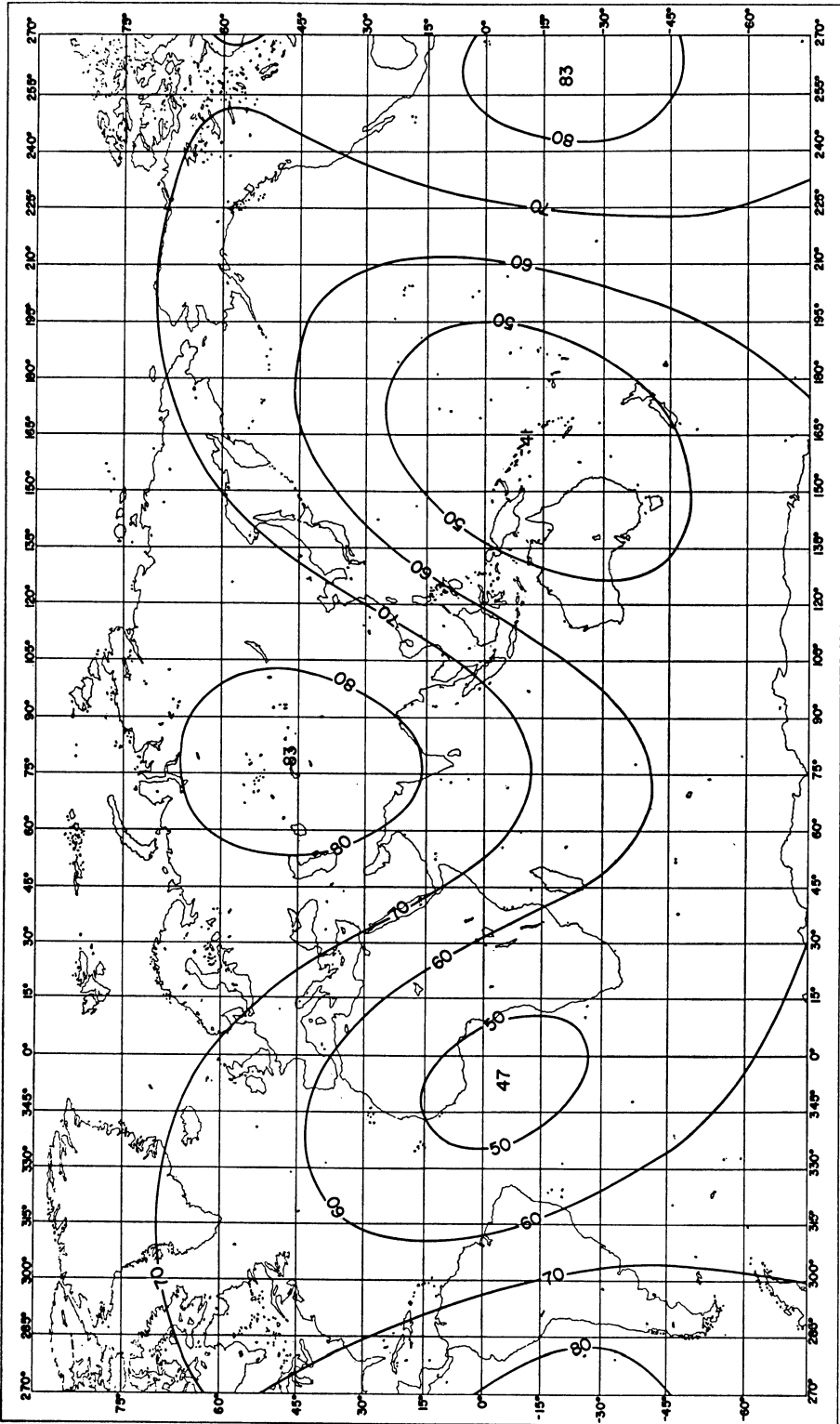


Fig. 4. Orthogonal function representation of all heat-flow values.

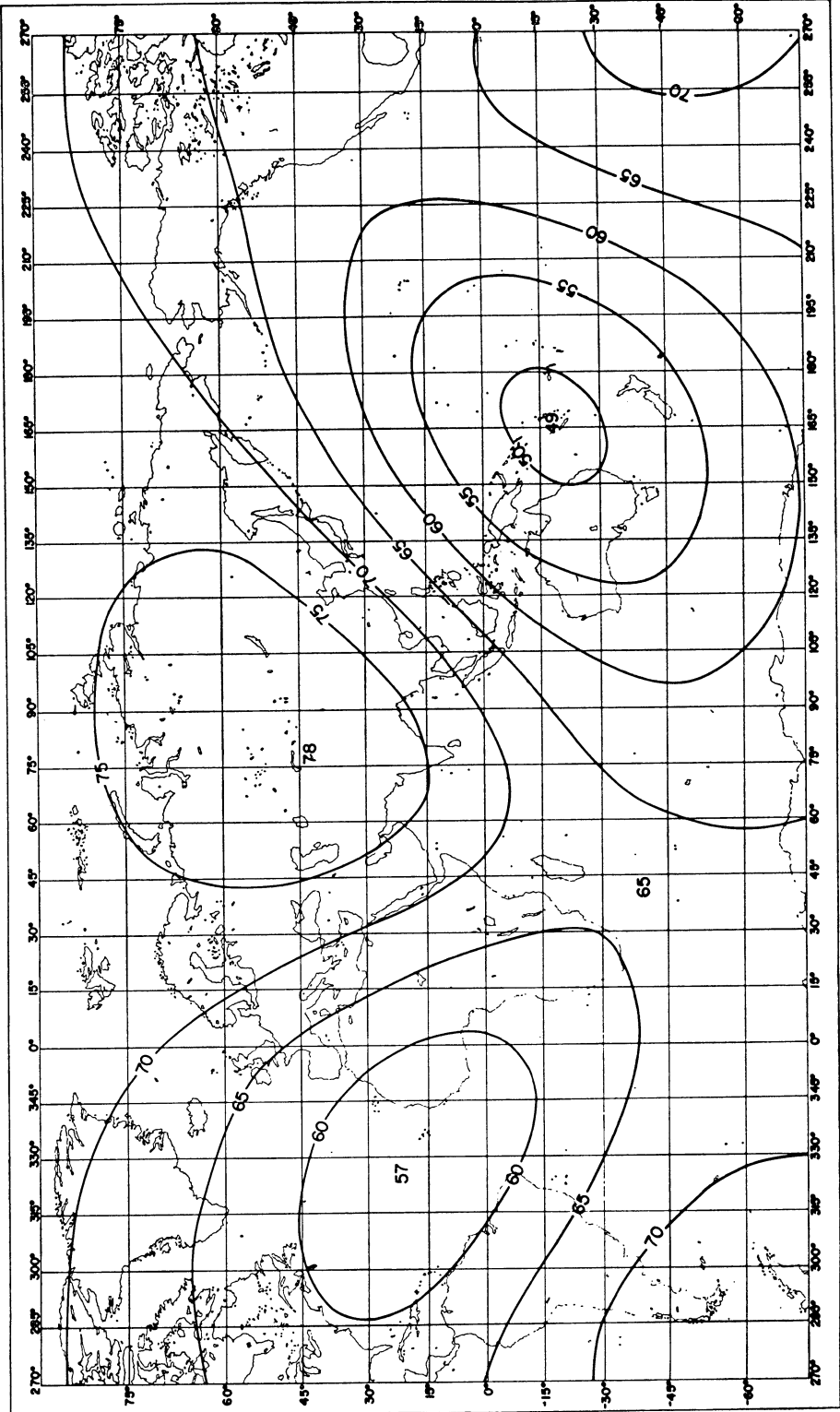


Fig. 5. Orthogonal function representation of weighted averages for the $5^\circ \times 5^\circ$ grid (see Figure 1).

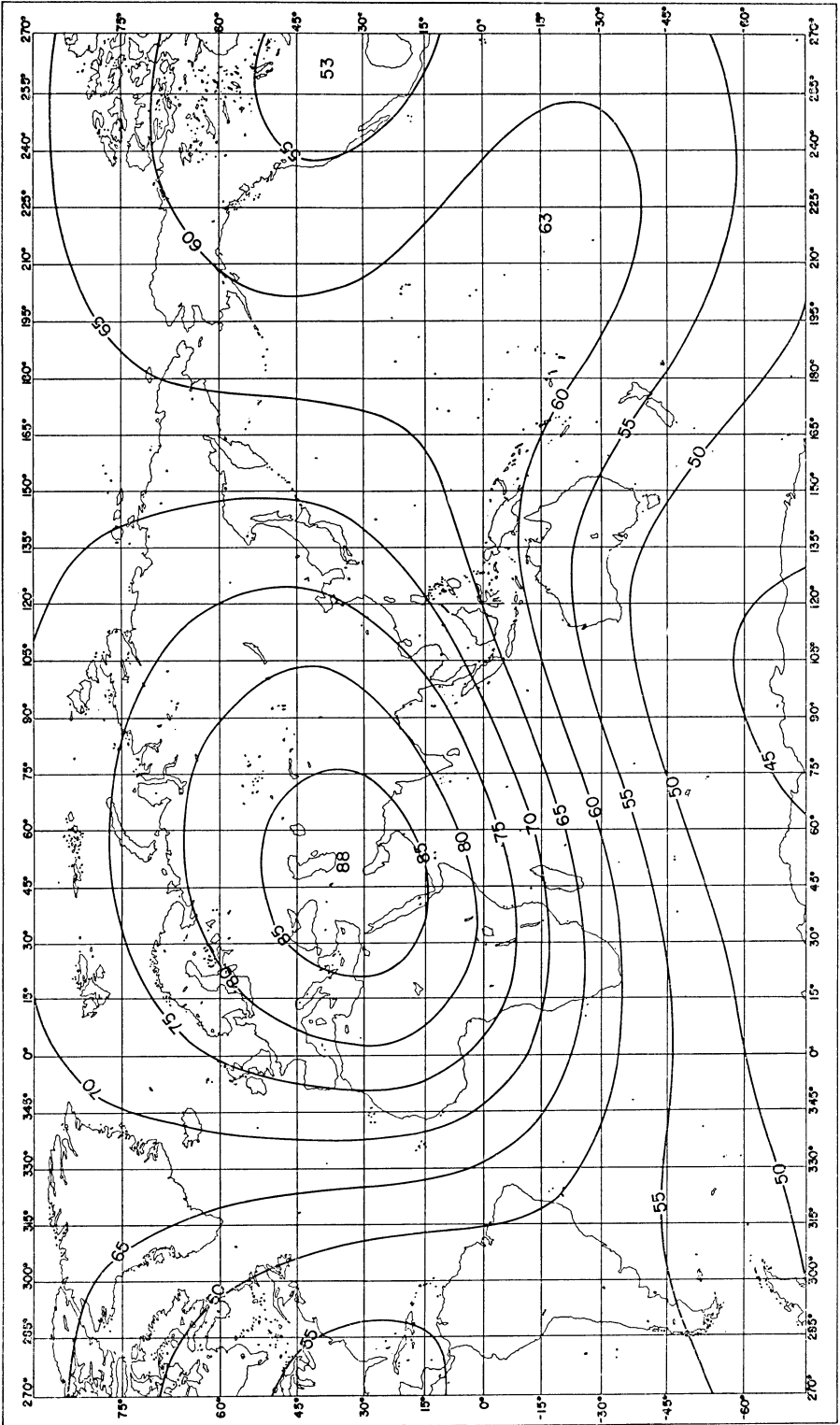


Fig. 6. Orthogonal function representation of weighted averages for the $45^\circ \times 45^\circ$ grid.

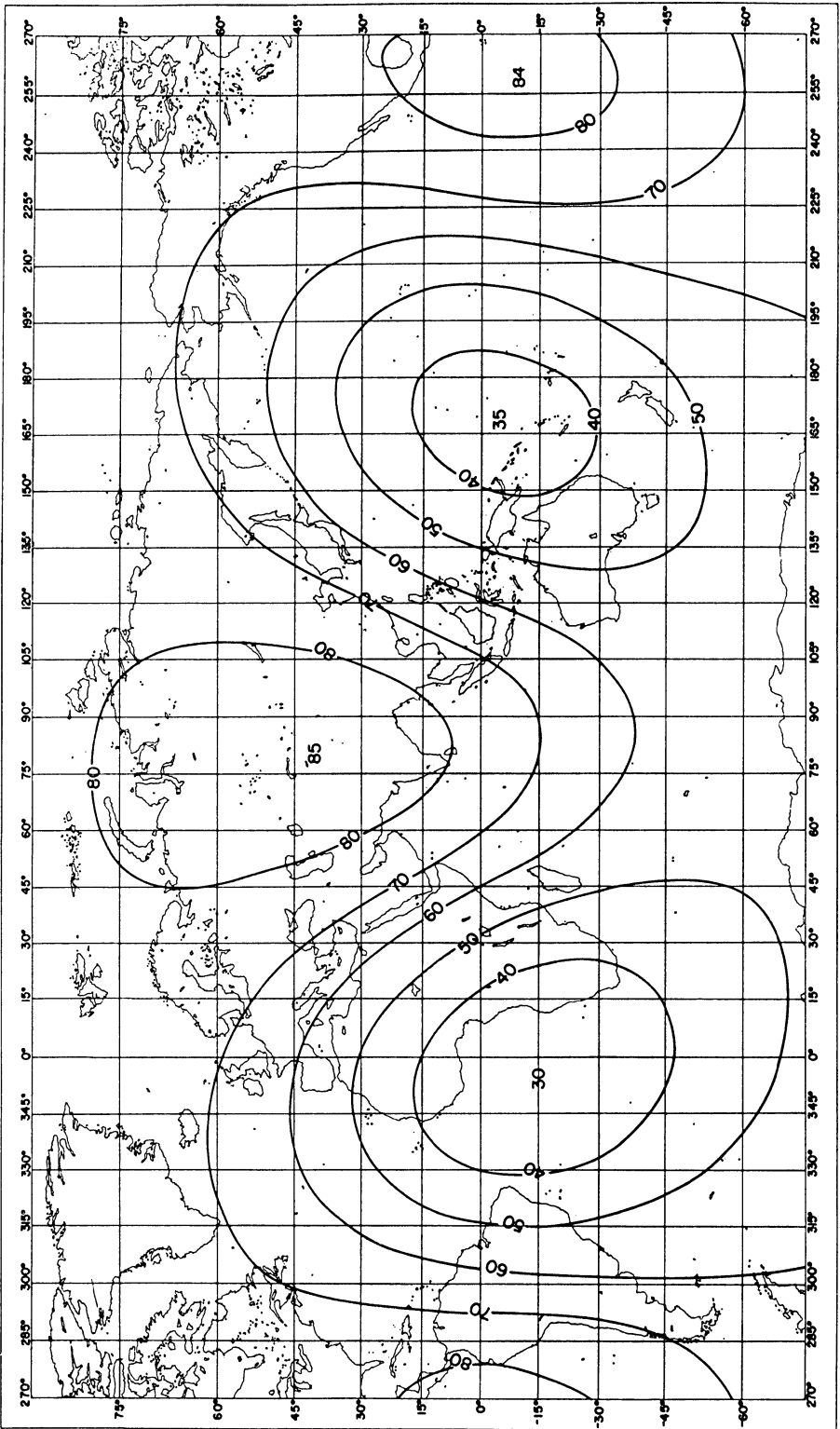


Fig. 7. Representation of 634 heat-flow values listed by Lee [1963] using all values.

TABLE 2. Coefficients in Spherical Harmonic Expansion

	Orthogonal Expansion, All Data	5° Weighted Averages	45° Weighted Averages	Extreme Values Deleted (611 Values)
a_0^0	63.95 (1.528)	63.97 (1.529)	63.13 (1.509)	58.66 (1.402)
a_1^0	3.01 (0.072)	1.62 (0.039)	6.36 (0.152)	1.03 (0.025)
a_1^1	1.19 (0.028)	2.46 (0.059)	3.02 (0.072)	-0.26 (-0.006)
a_2^0	2.26 (0.054)	2.39 (0.057)	-2.61 (-0.062)	2.42 (0.058)
a_2^1	0.19 (0.004)	-1.50 (-0.036)	1.76 (0.042)	-1.40 (-0.033)
a_2^2	7.85 (0.188)	-3.12 (-0.075)	1.24 (0.029)	-2.18 (-0.052)
b_1^1	-2.17 (-0.052)	1.33 (0.032)	4.17 (0.100)	1.36 (0.032)
b_2^1	4.41 (0.105)	3.58 (0.085)	4.73 (0.113)	2.03 (0.048)
b_2^2	3.37 (0.080)	1.61 (0.038)	2.20 (0.052)	1.62 (0.039)

The average value of the heat flow for continents and ocean basins can be obtained from the representations given in Figures 3, 4, and 5 through the use of the continentality function introduced by *Munk and MacDonald* [1960]. We multiply the coefficients of the spherical harmonics representing the heat flow as shown in Figures 4 to 6 by the continentality function to obtain the means for the continents and oceans in Table 1. The average over continental areas is higher than that over oceans, as is evident from Figures 4 to 6. The three representations give closely similar values, and we adopt a continental average of 69.0 erg cm⁻² sec⁻¹ (1.65) and an oceanic average of 62.0 erg cm⁻² sec⁻¹ (1.48).

Unlike the arithmetic averages, the orthogonal expansion gives higher values for the continental regions than for the oceanic regions. The difference between continents and oceans is not significant at the 95 per cent confidence level.

The representation of the heat flow shown in Figure 4 is based on the 757 values. An earlier representation using 634 heat-flow values, listed by *Lee* [1963], is given in Figure 7. The additional values lie in the South Atlantic and the western Pacific, etc., areas for which we had few or no data before. The principal features illustrated in Figures 4 through 6 also show up in Figure 7. The heat flow is low over the western Pacific; there is a high in the central Asian mass, a low in the eastern Atlantic, and a prominent high in the eastern Pacific off the coast of South America. The principal effect of the addition of the 123 values is to decrease

the amplitude of the heat-flow anomalies. However, the major features of the field remain.

Spherical harmonic coefficients. The spherical harmonic coefficients corresponding to the various representations are listed in Table 2. The normalization used is that in which the associated Legendre functions are those fully normalized in such a way that

$$\int (P_n^m)^2 d\sigma = 4\pi \tag{2}$$

where the integration is over the unit sphere [*Chapman and Bartels*, 1951]. The individual values in the coefficients vary somewhat among the various representations. However, in all of them the dominant term is the zeroth-order term, though there is significant power in the other coefficients.

The values for the spherical harmonic expansion of the field with the extreme values deleted are also shown in Table 2. The coefficients are very similar to those for the 5° weighted averages except for the zeroth-order term.

Table 3 lists the root mean square values of the surface harmonics defined by

TABLE 3. Mean Values of Surface Harmonics [1/4π ∫ σ(Y_n)² dσ]^{1/2}

Degree	Orthogonal Expansion, All Values	5° Weighted Averages	45° Weighted Averages
0	63.95 (1.528)	63.97 (1.529)	63.13 (1.509)
1	3.90 (0.093)	3.23 (0.077)	7.04 (0.168)
2	9.88 (0.236)	5.75 (0.137)	6.22 (0.149)

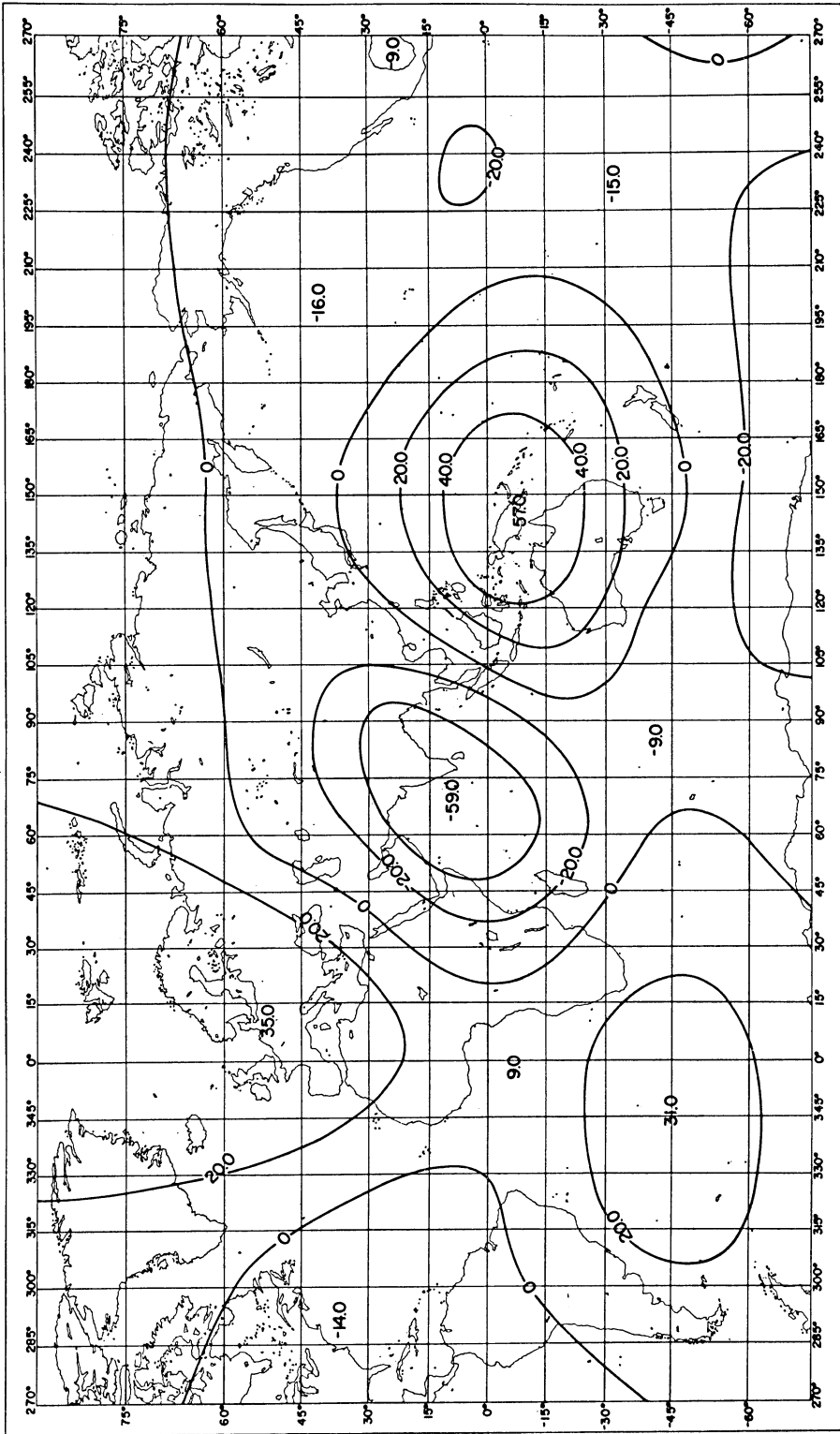


Fig. 8. Geoid heights in meters referred to the ellipsoid with a flattening of $1/298.3$ after *Kaula* [1963]. The geoid is derived from Baker-Nunn camera observations of satellites 1959 α , 1959 η , 1960 ν_2 , 1961 δ .

$$\left[\frac{1}{4\pi} \int_{\sigma} (Y_n)^2 d\sigma \right]^{1/2} \quad (3)$$

$$Y_n = \sum_{m=0}^n (a_n^m \cos m\lambda + b_n^m \sin m\lambda) P_n^m(\sin \theta)$$

If all values are used in the orthogonal expansion, there is a tendency for higher power to occur in the surface harmonics than if average values for areas are used. This may be an expression of the fact that the least-squares fit to the irregularly distributed station tends to overestimate individual coefficients since the least-squares fit distorts the harmonics in those regions for which observations are abundant.

Comparison with the gravitational field. Figure 8 shows the geoid derived by *Kaula* [1963] from a study of a number of artificial earth satellites. The geoid is referred to an ellipsoid with flattening 1/298.3. The principal anomalies lie in the western Pacific, centered on New Guinea where the geoid is high by about 57 meters and over India and the Indian Ocean where the geoid is depressed by a maximum of 59 meters. The gravity geoid anomalies correlate roughly with the features of the heat-flow field. The sense of the correlation is that where the heat flow is high the geoid is depressed, and vice versa. Thus, over the western Pacific, where the geoid is raised, the heat flow is lower than average. The correlation is not perfect, as would be expected because of the uncertainties both in the heat-flow and gravity fields.

The correlation between a low heat flow and a high in the geoid is in the sense expected if the anomalies in both fields are associated with convection motions within the mantle. A hot, rising column will have associated with it a deficiency in mass, and the column will carry an excess of heat. A descending column of the same vertical dimensions will contain a greater mass, and the heat flow should be lower than normal. It can be demonstrated by an order of magnitude calculation that the anomalies in the gravitational and heat-flow fields are consistent with convection currents having velocities of a few centimeters per year. We consider ascending and descending columns of the same vertical dimension L with a temperature difference ΔT . The mass difference between the two columns is

$$\rho \alpha \Delta T L \quad (4)$$

where ρ is density and α is coefficient of thermal expansion. The mass excess in (4) is expressed in terms of grams per unit area. The heat carried by such a convection system is of the order of $\rho c_p \Delta T v$, where c_p is the specific heat and v is the velocity. The ratio of the unknown velocity to the unknown vertical dimension L is given by

$$\frac{v}{L} = \frac{\alpha}{c_p} \frac{Q}{M} \quad (5)$$

where Q is the heat carried by the convection system and M is the excess mass. For the earth, the ratio α/c_p is about 10^{-12} . The heat-flow anomalies are of the order of $50 \text{ erg cm}^{-2} \text{ sec}^{-1}$, and the excess mass corresponding to an amplitude of 100 meters in the geoid is $3 \times 10^4 \text{ g cm}^{-2}$. With these numerical values, the velocity is

$$v = 5 \times 10^{-15} L \text{ sec}^{-1} \quad (6)$$

For vertical dimensions of the order of 1000 km, the vertical velocity would have to be about 15 cm year^{-1} . Alternatively, if the dimensions are of the order of 100 km, velocities of 1.5 cm year^{-1} would be consistent with the observed gravity and heat-flow anomalies.

In the scale analysis presented above a possible mass excess due to denser mantle material being pulled up by the rising current is neglected. *Licht* [1960], using the analysis of *Vening-Meinesz* [*Heiskanen and Vening-Meinesz*, 1958], finds that the geoid might indeed be high over a rising convection current. This result is based, however, on a detailed application of a theory in which a viscous fluid is assumed.

This preliminary study indicates the importance of measurements of surface heat flow in the central Asian mass, equatorial Africa, and South America where we have no data at present. Since the present heat-flow data are rather limited, spherical harmonics up to and including second orders were significant and were used in obtaining the representations of the heat-flow field. However, there is a possibility that the anomalies in the heat-flow field are actually much smaller-scale phenomena than those that can be represented by the low-order harmonics used in the representation.

Acknowledgments. We wish to thank Drs. T. Boldizar, M. G. Langseth, J. Reitzel, J. H. Sass, S. Uyeda, and R. P. Von Herzen for their kindness in supplying their unpublished data.

REFERENCES

- Blackman, R. B., and J. W. Tukey, *The Measurement of Power Spectra*, Dover Publications, New York, 1958.
- Bullard, E. C., The interior of the earth, in *The Earth as a Planet*, edited by J. P. Kuiper, pp. 105-122, University of Chicago Press, Chicago, 1954.
- Chapman, S., and J. Bartels, *Geomagnetism*, vol. 2, pp. 606-638, Clarendon Press, Oxford, 1951.
- Fougere, P., Spherical harmonic analysis, *J. Geophys. Res.*, 68, 1131-1139, 1963.
- Heiskanen, W. A., and F. A. Vening-Meinesz, *The Earth and Its Gravity Field*, chapter 11, McGraw-Hill Book Company, New York, 1958.
- Kaula, W. M., Statistical and harmonic analysis of gravity, *J. Geophys. Res.*, 64, 2401-2421, 1959.
- Kaula, W. M., Improved geodetic results from camera observations of satellites, *J. Geophys. Res.*, 68, 5183-5190, 1963.
- Lee, W. H. K., Heat flow data analysis, *Rev. Geophys.*, 1, 449-479, 1963.
- Licht, A. L., Convection currents in the earth's mantle, *J. Geophys. Res.*, 65, 349-353, 1960.
- Munk, W. H., and G. J. F. MacDonald, *Rotation of the Earth*, Cambridge University Press, Cambridge, 1960.
- Nason, R. D., and W. H. K. Lee, Preliminary heat flow profile across the Atlantic, *Nature*, 196, 975, 1962.
- Von Herzen, R. P., and S. Uyeda, Heat flow through the eastern Pacific Ocean floor, *J. Geophys. Res.*, 68, 4219-4250, 1963.

(Manuscript received August 14, 1963;
revised September 19, 1963.)